International Journal of Engineering and Geosciences
https://dergipark.org.tr/en/pub/ijeg
e-ISSN 2548-0960

Assessment of the solar energy potential of rooftops using LiDAR datasets and GIS based approach

Vancho Adjiski [*1], **Gordana Kaplan** [2], **Stojance Mijalkovski** [1]

[1]*Goce Delcev University, Faculty of natural and technical sciences, Macedonia*
[2]*Eskisehir Technical University, Institute of Earth and Space Sciences, Türkiye*

Keywords
LiDAR
GIS
Solar irradiation
Photovoltaic (PV) potential
Rooftop

Research Article
DOI: 10.26833/ijeg.1112274

Received: 03.05.2022
Accepted: 22.09.2022
Published: 19.10.2022

Abstract

The importance of solar energy as a global energy source is expected to grow. Solar power's future looks bright, especially with an aged and deteriorating energy grid and rising fossil fuel prices. More precise methods for assessment of solar capacity are needed as more homes and companies investigate the possibility of small-scale photovoltaic (PV) solar installations. In this study, a spatial solar energy PV potential assessment method based on the combination of LiDAR (Light Detection and Ranging) datasets and GIS (Geographic Information System) is proposed. The proposed methodology is applied to an area in the capital city of Skopje in N. Macedonia, from where the results of the possible annual energy output of PV systems for the selected rooftops were presented. The results of the study were presented in a map showing rooftops that are most suitable for installing PV systems. From this map, three random roofs were selected to perform manual estimates of the number of panels that could fit on them and the potential energy output of the solar PV systems. This study provides crucial results for financial and urban planning, policy formulation for future energy projects and also allows to analyze different mechanisms to promote PV installations on publicly available rooftops.

1. Introduction

Solar energy is the most abundant and cleanest renewable energy source. Because of its availability and long-term viability, solar energy is recognized as one of the most important renewable energy sources in the world [1-2]. The relevance of solar energy as a global energy source is expected to grow. Electricity from photovoltaic (PV) systems are expected to become increasingly essential in this scenario as performance improves, production costs decrease, and the cost of electricity from other sources rises [3]. Solar energy is also seen as a democratic energy source, with anyone able to explore and utilize it.

Unlike commercial sources such as fuel and coal, using renewable energies such as solar does not contribute to today's ever-increasing environmental challenge [4]. More countries are turning to use solar power to meet their energy needs, harnessing this high-potential energy source through PV systems, which converts sunlight into electricity [5].

According to the United Nations (UN), half of the world's population now lives in cities, which will rise to 60 % by the year 2050 [6]. As a result, developing urban plans that secure their long-term expansion should be a more significant problem. All countries' energy policies should prioritize promoting the transition to a new energy model based on efficient use of electricity and renewable energy sources [7]. The European Union (EU) has recommended a reform of the energy system to adapt to this situation. According to Directive 2009/28/EC, the EU shall achieve a minimum 25 % renewable energy share after 2025 [8].

Sustainable development refers to meeting current needs without jeopardizing future generations' ability to meet their own. There is an endeavor to reconcile environmental, economic, and social concerns within sustainable community development.

While this study focuses on the feasibility of solar PV systems as a means of reaching environmental targets for greenhouse gas reduction, there are additional social and economic considerations when examining the viability of

* **Corresponding Author**

*(vanco.adziski@ugd.edu.mk) ORCID ID 0000-0001-6401-6835
(kaplangorde@gmail.com) ORCID ID 0000-0001-7522-9924
(stojance.mijalkovski@ugd.edu.mk) ORCID ID 0000-0003-3352-2158

Cite this article

Adjiski, V., Kaplan, G. & Mijalkovski, S. (2023). Assessment of the solar energy potential of rooftops using LiDAR datasets and GIS based approach. International Journal of Engineering and Geosciences, 8(2), 188-199

solar energy. For numerous reasons, the study is limited to the solar energy potential of rooftops. Solar conversion technologies such as solar heating and solar PV are often implemented on building roofs [9-12]. Furthermore, the usage of these technologies on rooftops implies that they are being used on the existing area and do not require space that forgoes other opportunities [13].

For this reason, having a methodology that can estimate the sun irradiation of specific locations is critical. These roof potential measurements can help solar planners, installers, and property owners to save money and speed up the evaluation process for rooftops and "green" structures [14].

Active airborne remote sensing is increasingly being utilized to acquire high-resolution data that can be used to create urban models with various detail levels. A remote sensing technique based on LiDAR (Light Detection and Ranging) can be used for developing high-resolution 3D Digital Terrain Model (DTM) and Digital Surface Model (DSM) for the simulation of incoming solar radiation hitting the rooftops [15-18]. Furthermore, information about ambient temperature and attributes of the chosen solar systems must be included to produce the best results for PV potential estimations.

The main data used in this study was the 1 m spatial resolution LiDAR point cloud obtained from the Agency for Real Estate Cadastre of N. Macedonia [19] as well as data for the Typical Meteorological Year (TMY) from the European Union Joint Research Centre [20]. The LiDAR data is from an area in the capital city Skopje (Fig. 1). The processed LiDAR data was used to identify roof planes within the selected area and determine their suitability by measuring their area, slope, aspect, and other characteristics like shade. In order to predict the possible annual energy output of each roof within the selected area, this was paired with the irradiation data. The development of this kind of model, which combines the ability of GIS to correlate alphanumeric data with spatial data, has become a crucial tool for comprehending the territory and, as a result, has contributed to the development of true "smart cities".

This research aims to create a methodology based on publicly available data that will enable for large-scale assessments of roof spaces and the maximum capacity of solar PV panels that can be put throughout entire cities and neighborhoods.

Figure 1. The study area in city of Skopje, used for the analyses

2. Method

2.1. Tools and data

The free and open-source GIS software QGIS was used for most of the core analysis in this study [21-24]. To generate the urban 3D model and to calculate the solar potential, the following open-source plugins within QGIS were employed:

- LAStools: LiDAR data-processing tool for seamless processing of large amounts of points that represent the selected urban objects [25].
- The Urban Multi-scale Environmental Predictor (UMEP): a group of tools that can be used for various applications related to outdoor thermal comfort, urban energy consumption, climate change mitigation, etc. The following services from this open-source plugin were utilized [26]:
  - UMEP MetPreprocessor: this tool is used to convert the required temporal meteorological data into the UMEP format. The following variables are usually required as a minimum input: air temperature, relative humidity, barometric pressure, wind speed, incoming shortwave radiation and rainfall (if available), other variables can be supplied as well.
  - UMEP Wall Height and Aspect: this tool is used to calculate the orientations and heights of the facades of buildings from a DSM. Wall aspect is given in degrees where north facing wall pixel has a zero value. The output of this plugin is used in other UMEP plugins such as Solar Energy on Building Envelopes.
- The SEBE (Solar Energy on Building Envelopes) plugin (inside UMEP): this tool calculates pixel-wise

potential solar energy using ground and building DSM. SEBE is also able to estimate irradiance on building walls.
- UMEP Daily Shadow Pattern: this tool calculates the pixel-wise shadow analysis using ground and building DSM.

The Agency for Real Estate Cadastre has started conducting LiDAR scanning of the territory of N. Macedonia. The activities are implemented within the project entitles "LiDAR survey of the entire territory of Republic of Macedonia for creating precise DEM and other quantitative and qualitative analyses of the Earth surface" [19]. The project activities include the LiDAR scanning of part of the Republic of North Macedonia territory. Most important input data which form the backbone of the methodology are described as follows:

- LiDAR point cloud data from the selected area (file from The Agency for Real Estate Cadastre N. Macedonia).
- Digital Surface Model (DSM): topographic digital file with elevation data of the urban environment, including the elevations of urban elements and represents the earth's surface, including all objects on it such as buildings, vegetation or roads.
- Digital Terrain Model (DTM): digital file with elevation data of the ground (bare Earth), on which the urban environment is based.
- Weather Data: Detailed climate file of the study area. This file is in the form of Typical Meteorological Year (TMY), a collation of selected weather data for a specific location, listing hourly values of solar radiation and meteorological elements for a one-year period. This detailed climate file was obtained from the EU JRC using their online TMY tool. The data used in this study is an average from the years 2006 - 2015 and contains the air temperature, air pressure, wind speed, wind direction, humidity, global horizontal irradiance, direct normal irradiance and diffuse horizontal irradiance [27].

Fig. 2 depicts the workflow process using these tools and data for analyzing the solar PV energy potential based on an urban 3D model.

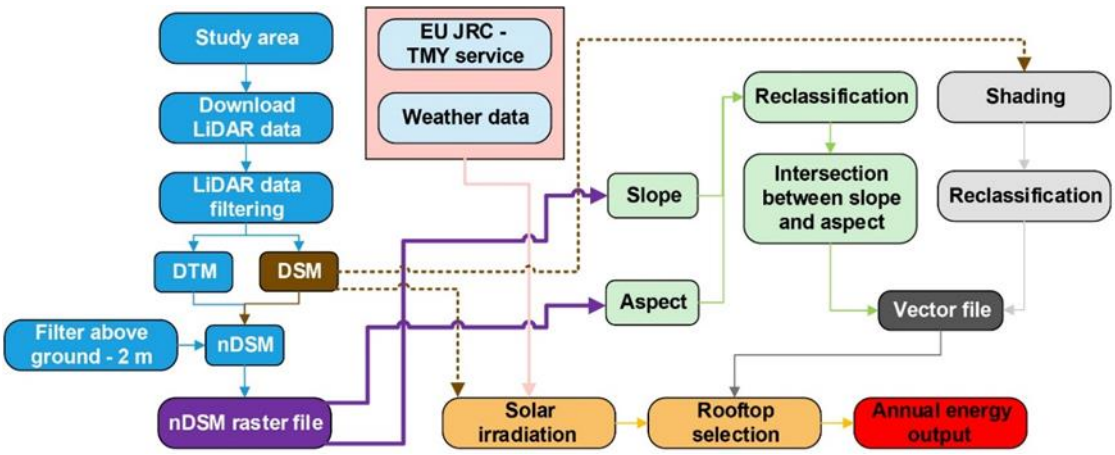

Figure 2. Proposed methodology for solar energy potential assessment

The methodology begins with the definition of the research area. The relevant LiDAR files (point cloud, DSM and/or DTM - depending on availability) are downloaded once the study area has been defined (download LiDAR data from The Agency for Real Estate Cadastre N. Macedonia). The LiDAR files must cover the entire research region. Prior to use, the LiDAR data (point cloud) must be filtered using LASTools (LiDAR data filtering) (Fig. 3a). A raster files containing only ground and building points is required due to this operation. This raster files represent greyscale images where the color of each pixel represents the elevation above sea level in meters. Two different forms of LiDAR images were generated in this process, a Digital Surface Model (DSM) (Fig. 3b) and a Digital Terrain Model (DTM) (Fig. 3c). A DTM contains only data for the bare ground, whereas a DSM contains elevation data for buildings, trees, and other surface structures. Both data sets have a spatial resolution of 1 m, implying that each pixel represents a 1 m^2 area.

A meteorological file is the final piece of data needed to do the solar analysis. The EU JRC provided this information via their online TMY service [27]. A TMY is a whole year's worth of meteorological data for a certain place on an hour by hour basis, including irradiance data. It is made up of averaging over several years to get the typical weather at any given period. The data used in this study is an average of air temperature, humidity, wind speed, wind direction, air pressure, global horizontal irradiance, direct normal irradiance, and diffuse horizontal irradiance for the years 2006 to 2015. This file must be formatted in a specified manner. First, from the EU JRC a Comma-Separated Values (CSV) file is downloaded. Second, in the UMEP MetPreprocessor tool, a matching between EU JRC weather data and UMEP meteorological parameters needs to be defined and performed. Finally, from the MetPreprocessor tool the UMEP meteorological file is obtained, which is then used in the SEBE tool.

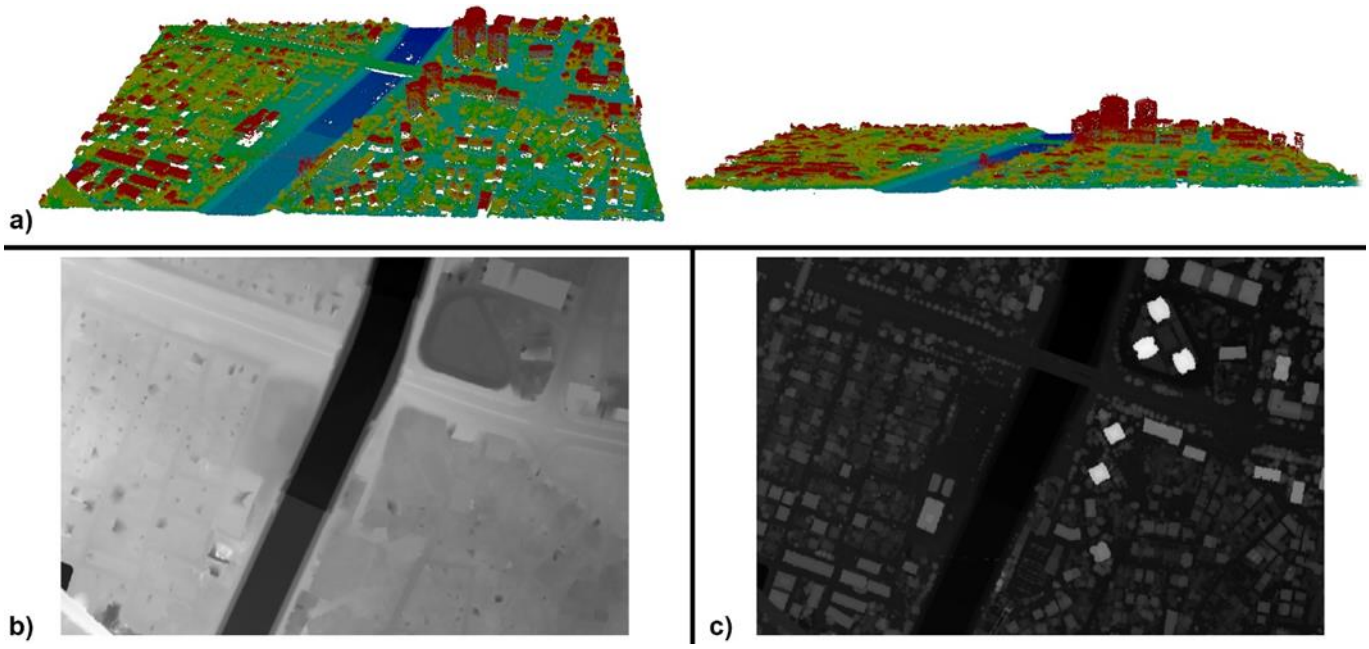

Figure 3. a) LiDAR 3D point cloud from the study area b) Digital Terrain Model (DTM) generated from the LiDAR 3D point cloud c) Digital Surface Model (DSM) generated from the LiDAR 3D point cloud

The next step of the proposed methodology in this study is to identify the potentially suitable roofs upon which a PV system could be installed.

The initial stage in this process was to generate a difference layer by subtracting the LiDAR DSM elevation values from the DTM elevation values. This results in a nDSM, or normalized DSM, which gives the elevation of surface features in meters above ground level rather than above sea level. This makes processing the roofs easier because a minimum height limit of 2 m (above the ground) can be set to filter out some of the ground characteristics. Fig. 4 shows the nDSM raster file with 2 m above the ground height limit filter.

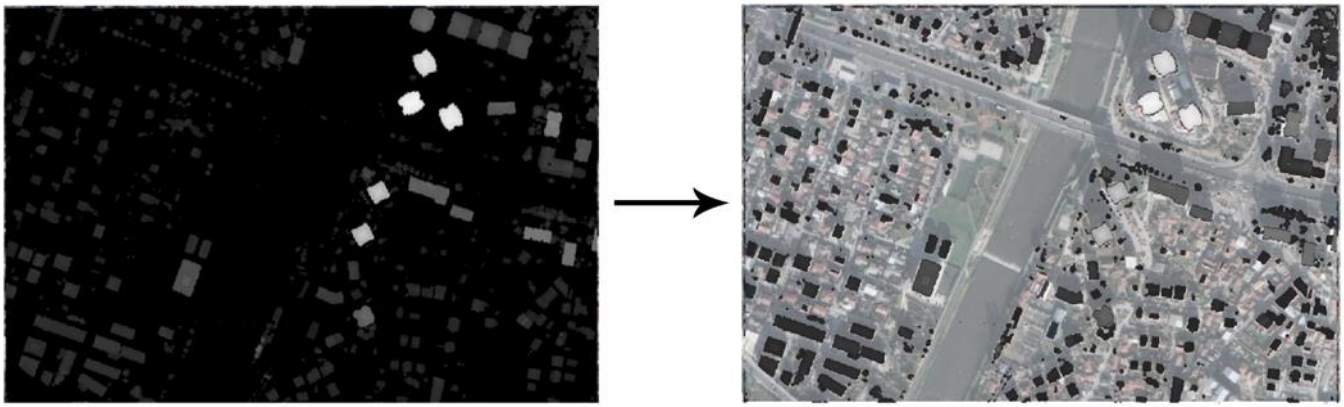

Figure 4. The nDSM raster file is shown on the left (subtract DTM from DSM). The right image, which is overlaid on aerial image from the study area, is obtained by applying a 2 m height filter.

The next step in this methodology is using LiDAR data in QGIS to analyze the slope and aspect of every roof in the study area. Using the built-in QGIS capabilities the height filtered nDSM was then used to construct an aspect raster and a slope raster, assigning each pixel an angle. The created aspect raster file represents an angular direction where black represents 0° (North) then each degree is assigned by shades of grey until looping around to white representing 360°. Each pixel has an angle assigned to it for the created slope raster file, with black representing 0° (flat) and white representing 90° (vertical). From these raster files, roof planes can be distinguished because they usually face a common direction and slope across the whole surface of the roof plane. Fig. 5a shows aspect raster file with the shades of grey represents a different angle, starting with black for North, through grey, and wrapping around to white. Fig. 5b shows slope raster file that represents a different angle, with the shades of grey starting with black for flat slopes and white for vertical slopes.

In order to identify the roof planes, the aspect raster was reclassified to 4 classes and the slope raster was reclassified to 3 classes in order to reduce the whole range of values. The classes are value ranges that the pixels in the raster's are assumed to have similar values. This permits regions with similar aspects and slopes to be grouped together. Fig. 6a and Fig. 6b depict this aspect and slope reclassification process.

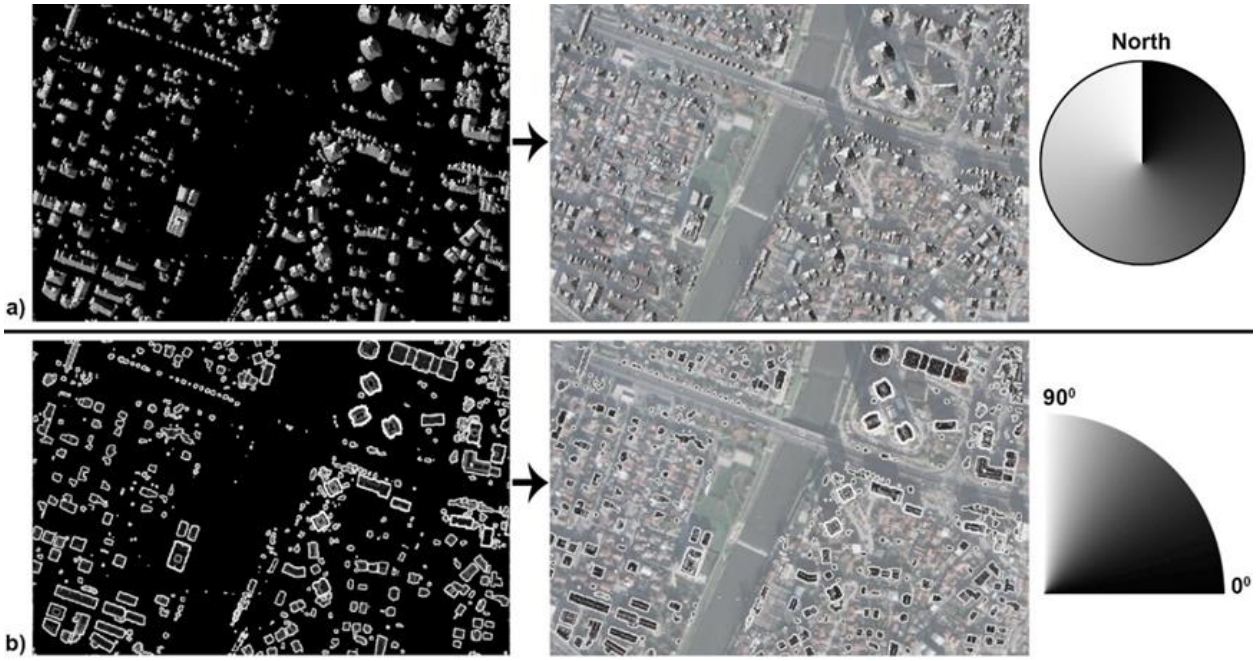

Figure 5. a) Aspect raster file created from the nDSM with shades of grey as color representation, starting with black for North, through grey, and wrapping around to white. b) Slope raster file created from the nDSM with shades of grey as color representation, starting with black for flat slopes, white for vertical slopes and grey in-between.

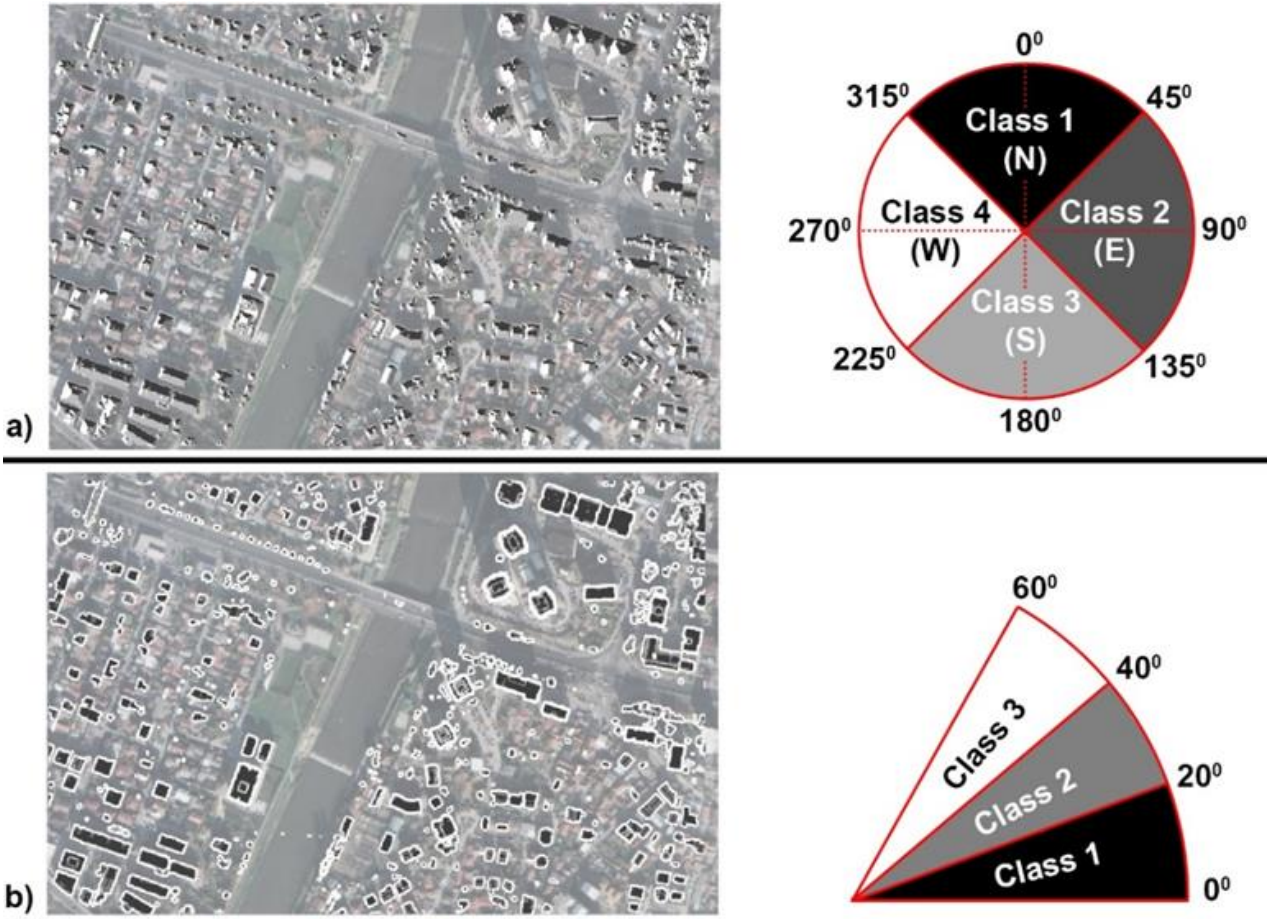

Figure 6. a) Aspect raster with 4 classes (N, E, S, W) by which each pixel was reclassified b) Slope raster with 3 classes by which each pixel was reclassified

Points with slopes greater than 60° were deleted because they were unsuitable for PV installation. Following reclassification, the aspect and slope raster's were filtered to eliminate noise using the Sieve tool in QGIS.

The QGIS Polygonise tool was then used to transform the aspect and slope raster's into vector polygons. This tool builds a polygon to represent the area of pixels by grouping together neighboring pixels with the same value. This format is significantly more useful because

the polygons may be saved as an ESRI Shapefile, which allows for the storage of the shape and position of each polygon as well as any additional attributes like aspect and slope that can be preserved as part of the database file.

Because roof planes share a common aspect and slope across their surface, the intersection of the aspect and slope polygons may be used to identify them. This intersection produces a new collection of shapes with a single aspect value and a single slope value representing roof planes. Fig. 7 shows the result of the intersection between the aspect and slope polygons.

Gathering information on each polygon shown in Fig. 7 such as accurate values for their aspect, slope, area, and location was the final stage in determining the roof planes. The latitude and longitude of each point were kept as an attribute of each shape in the database file, and QGIS was used to compute the center of each polygon. The Zonal Statistics tool in QGIS was used to determine the mean value for the aspect and slope of each roof plane, which allows for statistical computations involving a raster with a vector overlay layer. Circular statistics were used for the aspect data to get an accurate mean since the data is in circular form (0^0-360^0). QGIS was used to determine the planimetric area of each polygon and the true area, which was computed by correcting the planimetric area using the mean slope of each polygon to account for the roof planes' top down projection.

Shading can be a critical component in determining a solar PV system's output, therefore it must be taken into account. The shading analysis was conducted using the LiDAR DSM data from Fig. 3c since it allows for the consideration of shade from buildings as well as other tall objects such as trees and the landscape in general.

The DSM was used into the UMEP Daily Shadow Pattern tool in QGIS, which generates a raster image of the shadow pattern at any given moment, with 0 representing shaded areas and 1 representing bright areas.

The plugin was used to create a shadow pattern for every hour between dawn and sunset for 4 different days. The solstices and equinoxes were chosen as the 4 days to account for the whole range of the Sun's locations throughout the year. Specifically, the days were 20th March 2021, 21st June 2021, 23rd September 2021 and 22nd December 2021.

The generated hourly shadow raster's for each of the selected days were combined to create a continuous raster with values ranging from 0 to 1, where 0 means that is shaded and 1 is lit throughout the whole day. Fig. 8(a-d) depicts these daily shadow raster's.

Because summer days are more significant for energy generation than winter days, the allowed shade was determined differently for each day of the season to reflect the relative value of each day. A shade level of 50 % was found suitable for the days in March and September. A shade level of 40 % was found suitable for the day in June, and a shading level of 60 % was found suitable for the day in December. This suggests that pixels with a value of less than 0.5 for March and September, less than 0.4 for June, and less than 0.6 for December, could be regarded unacceptable for the daily shadow raster's shown in Fig. 8(a-d).

By reclassifying unsuitable pixels to a value of 0 and suitable pixels to a value of 1, these criteria were used to construct daily binary shadow raster's (Fig. 9a). Finally, the generated four binary raster (shown in Fig. 9a) were multiplied to form a single binary raster. This means that in order for a pixel to have a value of 1, it must have a value of 1 in each of the four raster's. Fig. 9b depicts the final shading raster, which can be used to determine whether the roof planes are suitable or not.

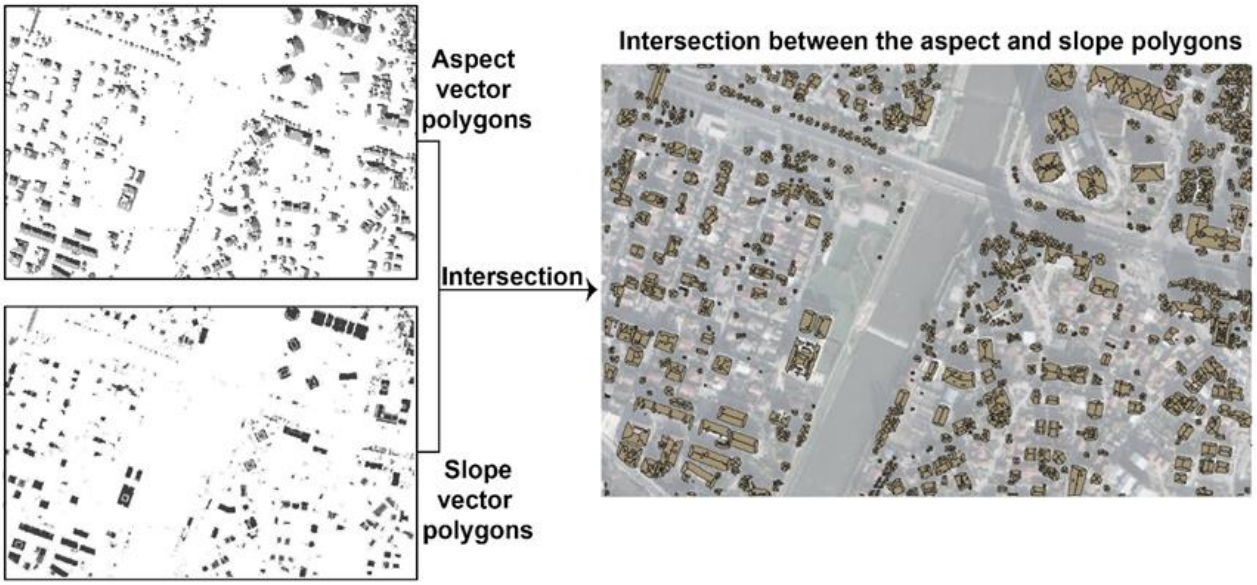

Figure 7. The intersection between the aspect and slope polygons representing roof planes with some additional surrounding artefacts

Figure 8. a) March shadow raster b) June shadow raster c) September shadow raster d) December shadow raster

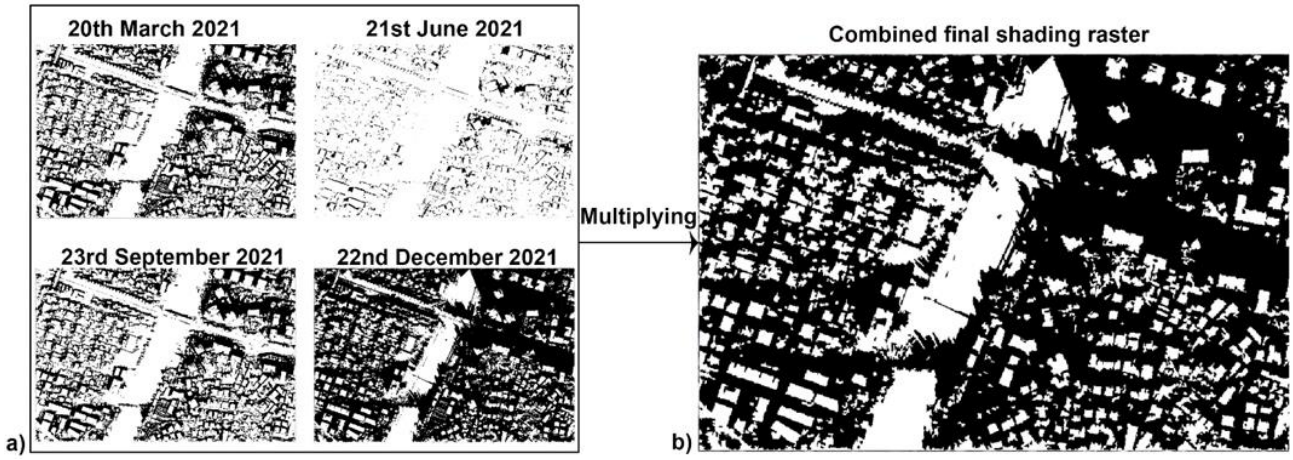

Figure 9. a) Binary shadow raster's where black pixel takes a value of 0 (unsuitable) and white pixels take a value of 1 (suitable) b) Combined final shading raster depicting the area locations which are suitable (white pixels) and unsuitable (black pixels) throughout the entire year

3. Results and Discussion

The first factor for a roof plane to be consider suitable was that it exceeded the minimum suitable area. In their study, Melius et al [28] characterized three approaches to assessing roof suitability: constant-value methods, manual selection, and GIS-based approaches. Most previous estimates of PV technical potential have relied on constant-value methods, which assume that a certain percentage of building rooftops can be used as PV areas, and these percentages are then applied to the total building stock to estimate the area available for PV systems [29-31]. Manual selection is based on visual clues such as aerial photography and Google Earth to determine the suitability of individual buildings for PV installations [32-33]. Methods based on GIS provide more precision than methods based on constant-value and can handle much larger data sets than methods based on manual selection [28]. In this paper, we used GIS-based method to provide a detailed analysis of the area available for PV system installations. A literature review was conducted and it was concluded that the minimum system size is a six-panel array which is equivalent to an area of around 10 m^2 [16,18,23]. Also, another factor must be considered: the buffer of minimum 0.5 m around the installed panels. As a result, considering the area of the panels and the buffer space between them a minimum roof area of 16 m^2 was chosen.

The potentially acceptable polygons were then filtered based on their slope and aspect. Following the reviewed literature, any polygon with a mean slope greater than 60° was ruled out as being too steep for a PV system to be installed [23].

The acceptable aspect range for pitched roofs was ENE through WNW or 67.5° to 292.5°, any roof outside this range was excluded. Fig. 10 shows a sample of the filtered, suitable roof planes represented by red polygons.

Figure 10. Identified red polygons that represent roof planes suitable for a solar PV system

The SEBE tools in UMEP was used to build a solar irradiation raster file, which was utilized to estimate the energy output of each roof [34]. This tool used the elevation data from the DSM and the weather and irradiance data from the TMY to generate the solar irradiation raster shown in Fig. 11. The output raster's units are in kWh, and because each pixel represents 1 m^2, the output is numerically equivalent to the average energy over an area of 1 m^2, expressed in kWh/m^2.

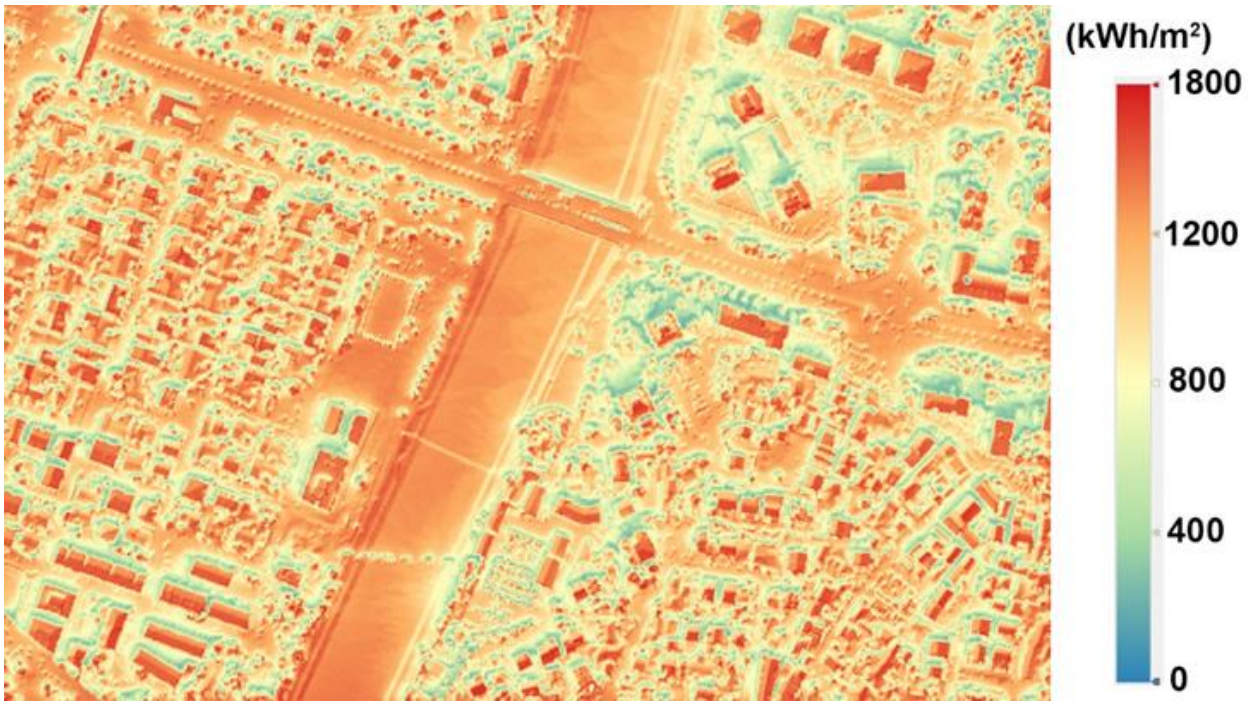

Figure 11. Annual solar irradiation raster from the study area

In order to make an assessment of the energy output of a rooftop solar PV system, the number of panels that could fit on each rooftop had to be estimated. This is a very difficult and time-consuming task to be performed manually for large-scale areas. Future work will include an extension of the research to deal with this process. The idea behind this step will be to develop an algorithm that can find the maximum number of rectangles that can fit inside any given shape.

In order to present the methodology, three random roofs were selected to have manual estimates of the number of panels that could fit on them (Fig. 12). For each of the selected roofs, a rectangular grid with the appropriate dimensions was generated to represent a solar array and the number of panels was then counted that could fit inside the roof polygon.

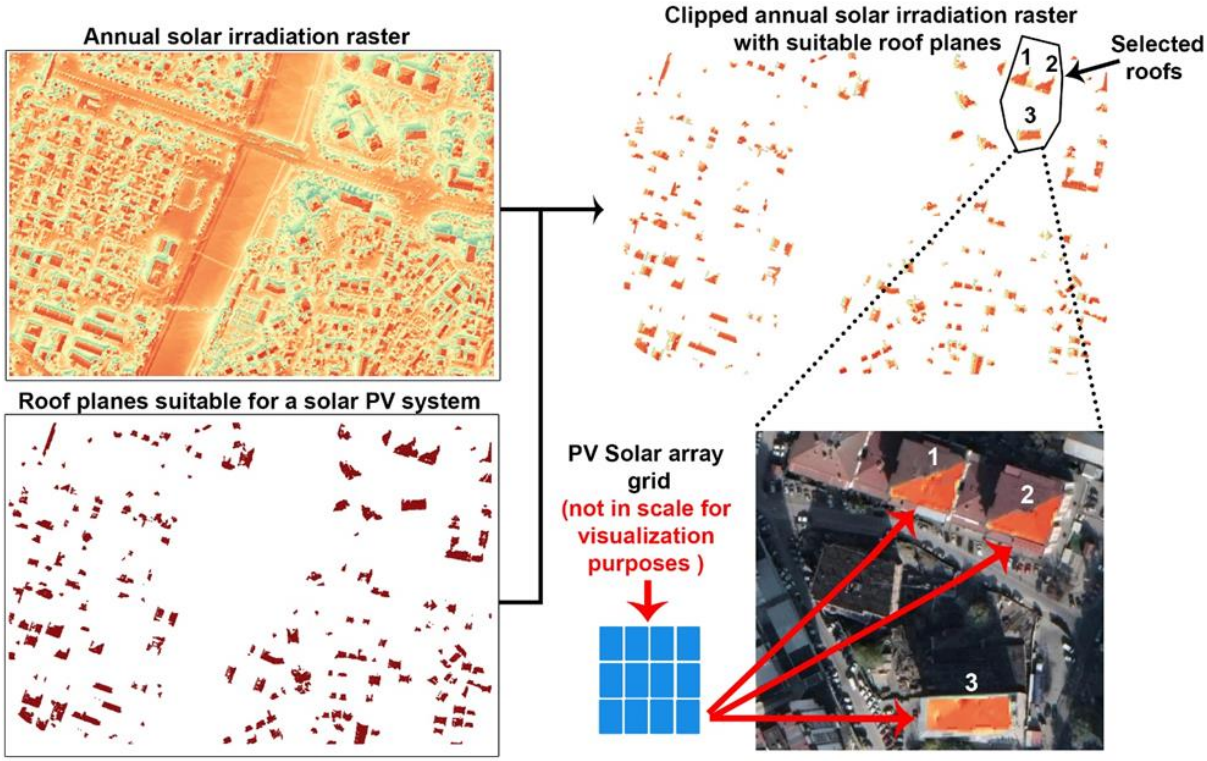

Figure 12. Manual panel number estimation for the selected roofs

The efficiency of the solar PV panels was the last variable to be determined in order to estimate the annual energy output for the selected roof.

The online EU PVGIS tool was used to calculate the average percentage loss for the selected location [27]. With a typical system loss of 14 %, the tool was used to determine the overall percentage loss for a 310 Wp (watt peak) yield crystalline silicon solar PV panel. The EU PVGIS online tool estimate an average overall loss of 22.9 % for the selected location in this study.

Now that the annual irradiation, number of panels, panel area, yield, and overall loss were estimated for each of the selected roofs, the annual energy production could be determined using the following term [35]:

$$E = A * N * r * H * PR \quad (1)$$

where:

E - annual energy output (kWh);

A - area of the solar panel (m^2);

N - number of panels for a given roof

r - solar panel yield or efficiency given by the ratio: electrical power (in kWp) of one solar panel divided by the area of one panel (%) (in this case this value is 0.18 %);

H - Annual mean irradiation for a given roof (kWh/m^2);

PR - Performance ratio, coefficient for losses (%) (this value is 0.77- takes into account the 22.9 % energy loss).

Equation (1) was applied to each of the selected rooftops to calculate the potential energy output if a solar PV system with the previously defined electrical characteristics were to be installed. The results are shown in Table 1.

Table 1. Potential energy output of a solar PV system for the selected rooftops in the study area

Roof ID	Roof area (m^2)	Number of panels	Area of one panel (m^2)	Area of the PV solar array grid (m^2)	Irradiation (kWh/m^2)	Energy output (kWh)
1	227	78	1.65	128.7	1416	25258
2	241	82	1.65	135.3	1434	26891
3	497	154	1.65	254.1	1372	50502

The results from Table 1 show the high potential energy output of a solar PV system for the selected rooftops. The calculated total annual energy output from the selected roofs was 102.6 MWh from 314 panels installed on 965 m^2 roof area. The results are promising and emphasize the fact there is good potential for residential solar PV energy production in N.Macedonia that have annual mean solar irradiation of 1450 kWh/m^2.

The results of the study are significant as remote sensing data and methods offer new techniques in many fields [36], and especially the use of Lidar data is getting more and more popular in the recent years [37-42].

4. Conclusion

Solar energy is one of the most promising ways for cities to shift to lower-carbon energy sources, so identifying potentially suitable roof spaces is vital for PV system deployment modeling.

Small area from the capital city Skopje in N. Macedonia was chosen as the study area. The analysis relied heavily on 1 m resolution aerial LiDAR point cloud for the selected area from the Agency for Real Estate Cadastre of N. Macedonia as well as data for the TMY for the selected area from the EU JRC.

The LiDAR data was used to locate roof planes in the study area and determine their suitability by measuring their area, slope, aspect, and other characteristics like shade. This was paired with the irradiation data. In order to predict the potential PV annual energy output, three randomly selected roofs were chosen from the study area.

Furthermore, the applicability of this assessment method can be used as a guide for solar energy utilization development plans in urban areas that can be extended to all appropriate infrastructure facilities.

The presented methodology in this study with the use of remote sensing, such as LiDAR, and GIS applications, has proven to be tools with extremely promising results. This type of research is expected to be extremely valuable for city energy planning because it allows for the assessment of PV solar energy potential of rooftops, which might account for a considerable portion of total building energy demand in cities.

The proposed method is repeatable, systematic, and based on high-resolution open-data sources and non-commercial software. The generated results offer high precision because are considering the 3D geometry of the buildings.

Acknowledgement

The authors would like to thank the Agency for Real Estate Cadastre of N. Macedonia for providing the LiDAR dataset.

Author contributions

Vancho Adjiski: Conceptualization, Methodology, Software, Writing-Original draft preparation, Visualization. **Gordana Kaplan:** Review, Writing-Review, Software-Verification. **Stojance Mijalkovski:** Checking draft and Editing.

Conflicts of interest

The authors declare no conflicts of interest.

References

1. Freitas, S., Catita, C., Redweik, P., & Brito, M.C. (2015). Modelling solar potential in the urban environment: state-of-the-art review. Renewable and Sustainable Energy Reviews, 41, 915-931.
2. Suri, M., Huld, T. A., Dunlop, E. D., & Ossenbrink, H. A. (2007). Potential of solar electricity generation in the European Union member states and candidate countries. Solar Energy, 81(10), 1295-1305. http://dx.doi.org/10.1016/j.solener.2006.12.007
3. Nwaigwe, K.N., Mutabilwa, P., & Dintwa, E. (2019). An overview of solar power (PV systems) integration into electricity grids. Materials Science for Energy Technologies, 2(3), 629-633. https://doi.org/10.1016/j.mset.2019.07.002.
4. Kåberger, T. (2018). Progress of renewable electricity replacing fossil fuels. Global Energy Interconnection, 1(1) 48-52. https://doi.org/10.14171/j.2096-5117.gei.2018.01.006.
5. Koo, C., Hong, T., Park, H.S., & Yun, G. (2014). Framework for the analysis of the potential of the rooftop photovoltaic system to achieve the net-zero energy solar buildings. Progress in photovoltaics: research and applications, 22(4), 462-478. https://doi.org/10.1002/pip.2448
6. United Nations, Department of Economic and Social Affairs, Population Division. (2014). World Urbanization Prospects: The 2014 Revision, Highlights, 32 p.
7. Lu, Y., Khan, Z.A., Alvarez-Alvarado, M.S., Zhang, Y., Huang, Z., & Imran, M. A. (2020). Critical Review of Sustainable Energy Policies for the Promotion of Renewable Energy Sources. Sustainability, 12(12), 1-30. https://doi.org/10.3390/su12125078
8. Directive 2009/28/EC of the European Parliament and of the Council of 23 April 2009 on the promotion of the use of energy from renewable sources and amending and subsequently repealing Directives 2001/77/EC and 2003/30/EC. Official Journal of the European Union L140. pp. 16–62.
9. Hong, T., Lee, M., Koo, C., Jeong, K., & Kim, J. (2017). Development of a method for estimating the rooftop solar photovoltaic (PV) potential by analyzing the available rooftop area using Hillshade analysis. Applied Energy, 194, 320-332. https://doi.org/10.1016/j.apenergy.2016.07.001
10. Bergamasco, L., & Asinari, P. (2011). Scalable methodology for the photovoltaic solar energy potential assessment based on available roof surface area: further improvements by ortho-image analysis and application to Turin (Italy). Solar Energy, 85(11), 2741-2756. https://doi.org/10.1016/j.solener.2011.08.010

11. Kodysh, J.B., Omitaomu, O.A., Bhaduri, B.L., & Neish, B.S. (2013). Methodology for estimating solar potential on multiple building rooftops for photovoltaic systems. Sustainable Cities and Society, 8, 31-41. https://doi.org/10.1016/j.scs.2013.01.002
12. Li, Y., Ding, D., Liu, C., & Wang, C. (2016). A pixel-based approach to estimation of solar energy potential on building roofs. Energy and Buildings, 129, 563-573. https://doi.org/10.1016/j.enbuild.2016.08.025
13. Adeleke, A.K., & Smit, J.L. (2016). Intergration of LiDAR data with aerial imagery for estimating rooftop solar photovoltaic potentials in city of Cape Town. ISPRS - International Archives of the Photogrammetry, Remote Sensing and Spatial Information Sciences, 41, 617-624.
14. Byrne, J., Taminiau, J., Kurdgelashvili, L., & Kim, K.N. (2015). A review of the solar city concept and methods to assess rooftop solar electric potential, with an illustrative application to the city of Seoul. Renewable and Sustainable Energy Reviews, Volume 41, 830-844. https://doi.org/10.1016/j.rser.2014.08.023.
15. Lukač, N., Žlaus, D., Seme, S., Žalik, B., & Štumberger, G. (2013). Rating of roofs' surfaces regarding their solar potential and suitability for PV systems, based on LiDAR data. Applied Energy, 102, 803-812. https://doi.org/10.1016/j.apenergy.2012.08.042
16. Jacques, D.A., Gooding, J., Giesekam, J.J., Tomlin, A.S., & Crook, R. (2014). Methodology for the assessment of PV capacity over a city region using low-resolution LiDAR data and application to the City of Leeds (UK). Applied Energy, 124, 28-34. https://doi.org/10.1016/j.apenergy.2014.02.076
17. Suomalainen, K., Wang, V., & Sharp, B. (2017). Rooftop solar potential based on LiDAR data: bottom-up assessment at neighbourhood level. Renewable Energy, 111, 463-475. https://doi.org/10.1016/j.renene.2017.04.025
18. Prieto, I., Izkara, J.L., & Usobiaga, E. (2019). The Application of LiDAR Data for the Solar Potential Analysis Based on Urban 3D Model. Remote Sensing, 11(20), 2348-2358. https://doi.org/10.3390/rs11202348
19. https://www.katastar.gov.mk/
20. European Union Joint Research Centre, "Typical Meteorological Year" (2017). [Online]. Available: https://re.jrc.ec.europa.eu/tmy.html (Date of access: 15 03 2022).
21. Latif, Z. A., Zak,i N. A. M., & Salleh, S. A. (2012). GIS-based estimation of rooftop solar photovoltaic potential using LiDAR. 2012 IEEE 8th International Colloquium on Signal Processing and its Applications, 2012, 388-392. https://doi.org/10.1109/CSPA.2012.6194755.
22. Suri, M., & Hofierka, J. (2004). A new GIS-based solar radiation model and its application to photovoltaic assessments. Transactions in GIS, 8(2), 175-190. https://doi.org/10.1111/j.1467-9671.2004.00174.x
23. Margolis, R., Gagnon, P., Melius, J., Phillips, C., & Elmore, R. (2017). Using GIS-based methods and LiDAR data to estimate rooftop solar technical potential in US cities. Environmental Research Letters, 12(7), 1-10. https://doi.org/10.1088/1748-9326/aa7225
24. Palmer, D., Koumpli, E., Cole, I., Gottschalg, R., & Bettts, T. (2018). A GIS-Based Method for Identification of Wide Area Rooftop Suitability for Minimum Size PV Systems Using LiDAR Data and Photogrammetry. Energies, 11(12), 1-22. https://doi.org/10.3390/en11123506
25. Rapidlasso GmbH LAStools. Available online: https://rapidlasso.com/lastools/ (Date of access: 15 03 2022).
26. Lindberg, F., Grimmond, C., Gabey, A., Jarvi, L., Kent, C., Krave, N., Sun, T., Wallenberg, N., & Ward, H. (2019). Urban Multi-scale Environmental Predictor (UMEP) Manual. University of Reading UK, University of Gothenburg Sweden, SIMS China, [Online] Available: https://umep-docs.readthedocs.io. (Date of access: 15 03 2022).
27. European Union Joint Reasearch Centre, Photovoltaic Geographical Reference System. (2017). [Online]. Available:https://re.jrc.ec.europa.eu/pvg_tools/en/tools.html (Date of access: 15 03 2022).
28. Melius, J., Margolis, R., & Ong, S. (2013). Estimating Rooftop Suitability for PV: A Review of Methods, Patents, and Validation Techniques. Golden (CO): National Renewable Energy Laboratory; 2013 December. Report No.: NREL/TP-6A20-60593.
29. Chaudhari, M., Frantzis, L., & Hoff, T.E. (2004). PV Grid Connected Market Potential Under a Cost Breakthrough Scenario. EF-Final-September 2004-117373 (Chicago: Navigant Consulting).
30. Frantzis, L., Graham, S., & Paidipati, J. (2007). California Rooftop Photovoltaic (PV) Resource Assessment and Growth Potential by County. CEC-500–2007-048 (Chicago: Navigant Consulting).
31. Paidipati, J., Frantzis, L., Sawyer, H., & Kurrasch, A. (2008). Rooftop Photovoltaics Market Penetration Scenarios. NREL/SR- 581–42306 (Golden, CO: National Renewable Energy Laboratory). https://doi.org/10.2172/924645
32. Ordonez, J., Jadraque, E., Alegre, J., & Martinez, G. (2010). Analysis of the photovoltaic solar energy capacity of residential rooftops in Andalusia (Spain). Renewable and Sustainable Energy Reviews,14, 2122-2130. https://doi.org/10.1016/j.rser.2010.01.001
33. Zhang, X., Walker, R., Salisbury, M., Hromiko, R., & Schreiber, J. (2009). Creating a Solar City: Determining the Potential of Solar Rooftop Systems in the City of Newark. Newark, DE: University of Delaware, Center for Energy and Environmental Policy.
34. Lindberg, F., Jonsson, P., Honjo, T., & Wästberg, D. (2015). Solar energy on building envelopes – 3D modelling in a 2D environment. Solar Energy, 115, 369-378. https://doi.org/10.1016/j.solener.2015.03.001.
35. Boyd, A. (2019). Mapping Solar PV Potential in Ambleside. Centre for Global Eco-Innovation, Joint report between CAfS and Lancaster University, 1-32.
36. Senkal, E., Kaplan, G., & Avdan, U. (2021). Accuracy assessment of digital surface models from unmanned aerial vehicles' imagery on archaeological sites.

International Journal of Engineering and Geosciences, 6(2), 81-89.
37. Diaz, B. S., Mata-Zayas, E. E., Gama-Campillo, L. M., Rincon-Ramirez, J. A., Vidal-Garcia, F., Rullan-Silva, C. D., & Sanchez-Gutierrez, F. (2022) LiDAR modeling to determine the height of shade canopy tree in cocoa agrosystems as available habitat for wildlife. International Journal of Engineering and Geosciences, 7(3), 283-293.
38. Özdemir, S., Akbulut, Z., Karsli, F., & Acar, H. (2021). Automatic extraction of trees by using multiple return properties of the lidar point cloud. International Journal of Engineering and Geosciences, 6(1), 20-26.
39. Sevgen, S. C. (2019). Airborne lidar data classification in complex urban area using random forest: a case study of Bergama, Turkey. International Journal of Engineering and Geosciences, 4(1), 45-51.
40. Özendi, M. (2022). Kültür varlıklarının yersel lazer tarama yöntemi ile dijital dokümantasyonu: Zonguldak Uzun Mehmet Anıtı örneği. Geomatik, 7 (2), 139-148. https://doi.org/10.29128/geomatik.917528
41. Yakar, İ., Çelik, M. Ö., Hamal, S. N. G. & Bilgi, S. (2021). Kültürel Mirasın Dokümantasyonu Çalışmalarında Farklı Yazılımların Karşılaştırılması: Dikilitaş (Theodosius Obeliski) Örneği. Geomatik, 6 (3), 217-226. https://doi.org/10.29128/geomatik.761475
42. Keleş, M. D. & Aydın, C. C. (2020). Mobil Lidar Verisi ile Kent Ölçeğinde Cadde Bazlı Envanter Çalışması ve Coğrafi Sistemleri Entegrasyonu-Ankara Örneği. Geomatik, 5 (3), 193-200. https://doi.org/10.29128/geomatik.643569